

NuTeV $\sin^2 \theta_W$ anomaly and nuclear parton distributions revisited

K. J. Eskola¹ and H. Paukkunen²

Department of Physics, P.B. 35, FIN-40014 University of Jyväskylä, Finland

Helsinki Institute of Physics, P.B. 64, FIN-00014 University of Helsinki, Finland

Abstract

By studying the Paschos-Wolfenstein (PW) ratio of deep inelastic νFe and $\bar{\nu}\text{Fe}$ scattering cross sections, we show that it should be possible to explain the NuTeV $\sin^2 \theta_W$ anomaly with quite conventional physics, by introducing mutually different nuclear modifications for the valence- u and valence- d quark distributions of the protons in iron. Keeping the EKS98 nuclear modifications for $u_V + d_V$ as a baseline, we find that some 20-30 % nuclear modifications to the u_V and d_V distributions account for the change induced in the PW ratio by the NuTeV-suggested increase $\Delta \sin^2 \theta_W = 0.005$. We show that introduction of such nuclear modifications in u_V and d_V individually, does not lead into contradiction with the present global DGLAP analyses of the nuclear parton distributions, where deep inelastic lA scattering data and Drell-Yan dilepton data from pA collisions are used as constraints. We thus suggest that the NuTeV result serves as an important further constraint in pinning down the nuclear effects of the bound nucleon PDFs. We also predict that if the NuTeV anomaly is explained by this mechanism, the NOMAD experiment should see an increase in the weak mixing angle quite close to the NuTeV result.

¹kari.eskola@phys.jyu.fi

²hannu.paukkunen@phys.jyu.fi

1 Introduction

A few years ago, the NuTeV collaboration at Fermilab reported that their measurements in deep inelastic neutrino-iron scattering indicate the value of Weinberg weak mixing angle $\sin^2 \theta_W = 0.2277 \pm 0.0013(\text{stat}) \pm 0.0009(\text{syst})$ [1]. This result was surprising, being about 3σ above the world average $\sin^2 \theta_W = 0.2227 \pm 0.00037$ [2]. A number of possible solutions to this deviation — the ‘NuTeV anomaly’ — has been proposed, ranging from conventional explanations within the Standard Model (SM) to more exotic ones requiring novel, beyond-SM, physics. For reviews, see Refs. [3, 4]. Today, the NuTeV anomaly is still an open problem calling for an answer.

As intriguing it would be to see new physics appearing, it is obviously crucial to first investigate in detail whether the explanation could be hidden in the features of parton distribution functions (PDFs) of the free and bound nucleons which are not yet fully known. For instance, the possible local asymmetry between strange and antistrange quark distributions, $S^- \equiv \int dx x [s(x) - \bar{s}(x)] \neq 0$ [5, 6, 7], and isospin violating PDFs [5, 7] may both be viable candidates for explaining the anomaly. Also the PDFs of bound nucleons, the nuclear parton distributions (nPDFs), have been considered as a source for the NuTeV anomaly [8]; for a review, see [3]. In particular the nuclear effects in the valence quark distributions u_V and d_V individually, have been thoroughly investigated in a global DGLAP analysis where the deep inelastic lA scattering (DIS) cross sections, the Drell-Yan (DY) dilepton cross sections in pA collisions and sum rules are used as constraints [9, 10, 11, 12]. Typically, however, the effects of the nPDFs, especially the differences of nuclear modifications in u_V relative to those in d_V , have been found to be too small to account for the NuTeV anomaly.

In this paper, we consider the NuTeV anomaly and the nPDFs from a new angle, taking the NuTeV result as an additional data constraint for disentangling the nuclear effects of u_V and d_V distributions in nucleons (protons) of iron. First, adopting the EKS98 global analysis of nPDFs [13] as a baseline, we examine in a rough but transparent way, how large nuclear effects relative to the EKS98 modification of $u_V + d_V$ in a proton of iron would be needed to fully account for the NuTeV anomaly. Nuclear modifications for u_V and d_V deviating from the EKS98 at most on a $\sim 30\%$ level (at the average NuTeV scale $Q^2 = 20.5 \text{ GeV}^2$) turn out to be sufficient.

Second, armed with the nuclear modifications for u_V and d_V individually, we recompute the DIS and DY cross sections, the data on which constrain the EKS98 modifications. Relative to the cross sections computed with EKS98, we find less than one percent changes for iron. This insensitivity shows that there can be fairly large differences between the nuclear effects in u_V and d_V which the standard global nPDF analyses [13, 9, 11] cannot disentangle. It also demonstrates the possible role of the NuTeV result as a new, orthogonal, constraint in pinning down the individual nuclear effects in the u_V and d_V distributions of bound nucleons. Not forgetting the other possible PDF-based explanations of the NuTeV anomaly, we thus suggest that a large part, if not all, of the NuTeV anomaly can be explained by introducing mutually different nuclear modifications for valence u and d quark distributions of protons in iron.

Third, as a consequence and a test of our hypothesis, we apply the obtained nuclear valence quark modifications to the neutrino cross sections measured in the NOMAD experiment at CERN [14]. We predict that the nonidentical nuclear effects in u_V and d_V induce a change in the ratio of neutral-to-charged current cross sections which, if identical nuclear effects were used, would correspond to an increase in $\sin^2 \theta_W$ quite close to that obtained by NuTeV.

The rest of the paper is organized as follows: In Sec. 2, we define the neutrino cross sections and structure functions in terms of PDFs, as well as the Paschos-Wolfenstein (PW) ratio we study. In Sec. 3, we define the nPDFs and show how the nuclear u_V and d_V distributions enter the PW ratio. We also show analytically the direction to which the nuclear effects in u_V and d_V should deviate relative to the modification of $u_V + d_V$ from EKS98. The results we obtain for individual nuclear modifications of u_V and d_V are presented in Sec. 4 both for the case where the NuTeV anomaly is fully explained and for the case where a third of the anomaly is accounted for. Section 5 contains the discussion on the DIS and DY cross sections. The NOMAD prediction is made in Sec. 6, and a brief outlook is given in Sec. 7.

2 Cross sections and Paschos-Wolfenstein ratio

We define the framework through the following well-known charged current (CC) and neutral current (NC) DIS cross sections of neutrinos and antineutrinos off a nucleus. In particular, we shall discuss the Paschos-Wolfenstein (PW) ratio [15]. In terms of double differential cross sections, the PW ratio is

$$R_A^-(x, Q^2) \equiv \frac{d\sigma_A^{\nu, \text{NC}}/dx dQ^2 - d\sigma_A^{\bar{\nu}, \text{NC}}/dx dQ^2}{d\sigma_A^{\nu, \text{CC}}/dx dQ^2 - d\sigma_A^{\bar{\nu}, \text{CC}}/dx dQ^2}, \quad (1)$$

where x and Q^2 are the standard Bjorken DIS variables, and A denotes the target. In studying the consequences of the NuTeV $\sin^2 \theta_W$ anomaly quantitatively, we shall focus on the PW ratio of x -integrated cross sections at a fixed scale Q^2 ,

$$R_A^-(x) \equiv \frac{d\sigma_A^{\nu, \text{NC}}/dQ^2 - d\sigma_A^{\bar{\nu}, \text{NC}}/dQ^2}{d\sigma_A^{\nu, \text{CC}}/dQ^2 - d\sigma_A^{\bar{\nu}, \text{CC}}/dQ^2}. \quad (2)$$

The neutral current cross section of a deep inelastic scattering of a neutrino (antineutrino) off a proton is [16]

$$\begin{aligned} \frac{d\sigma^{\nu(\bar{\nu}), \text{NC}}}{dx dQ^2} &= \frac{G_F^2}{\pi} \left(\frac{M_Z^2}{M_Z^2 + Q^2} \right)^2 \frac{1}{8x} \left[xy^2 F_1^{\nu(\bar{\nu}), \text{NC}}(x, Q^2) \right. \\ &\quad \left. + (1 - y - \frac{mxy}{2E}) F_2^{\nu(\bar{\nu}), \text{NC}}(x, Q^2) \pm xy(1 - \frac{y}{2}) F_3^{\nu(\bar{\nu}), \text{NC}}(x, Q^2) \right], \end{aligned} \quad (3)$$

where y is one of the standard Bjorken DIS variables and E is the (anti)neutrino beam energy. For these DIS variables $Q^2 = 2xymE$, where m is the mass of a nucleon. We

shall use here $m = 940$ MeV both for protons and for neutrons. The Z -boson mass is $M_Z = 91.1876$ GeV, and the Fermi coupling constant $G_F = 1.16637 \cdot 10^{-5}$ GeV $^{-2}$, taken from [16]. The structure functions are in the leading order expressed in terms of the quark and antiquark number densities in the free proton as

$$F_1^{\nu, \text{NC}}(x, Q^2) = F_1^{\bar{\nu}, \text{NC}}(x, Q^2) = \sum_{q=u,d,s,c,b} (R_q^2 + L_q^2) [q(x, Q^2) + \bar{q}(x, Q^2)] \quad (4)$$

$$F_2^{\nu, \text{NC}}(x, Q^2) = F_2^{\bar{\nu}, \text{NC}}(x, Q^2) = 2x F_1^{\nu, \text{NC}}(x, Q^2) \quad (5)$$

$$F_3^{\nu, \text{NC}}(x, Q^2) = F_3^{\bar{\nu}, \text{NC}}(x, Q^2) = 2 \sum_{q=u,d} (L_q^2 - R_q^2) q_V(x, Q^2), \quad (6)$$

where, as usual, $L_q = \tau_3 - 2e_q x_W$ and $R_q = -2e_q x_W$. The weak mixing angle is $x_W \equiv \sin^2 \theta_W$, the quark's electric charge is e_q and its third component of the weak-isospin is τ_3 . All quarks are treated as massless here, as is usually the case in the DGLAP-evolved PDFs we shall apply below. The valence quark distribution is defined as $q_V(x, Q^2) \equiv q(x, Q^2) - \bar{q}(x, Q^2)$.

The charged current deep inelastic cross section of a neutrino (antineutrino) scattering off a proton can be expressed in a similar manner [16],

$$\begin{aligned} \frac{d\sigma^{\nu(\bar{\nu}), \text{CC}}}{dx dQ^2} &= \frac{G_F^2}{\pi} \left(\frac{M_W^2}{M_W^2 + Q^2} \right)^2 \frac{1}{2x} \left[xy^2 F_1^{\nu(\bar{\nu}), \text{CC}}(x, Q^2) \right. \\ &\quad \left. + (1 - y - \frac{mxy}{2E}) F_2^{\nu(\bar{\nu}), \text{CC}}(x, Q^2) \pm xy(1 - \frac{y}{2}) F_3^{\nu(\bar{\nu}), \text{CC}}(x, Q^2) \right]. \end{aligned} \quad (7)$$

For the W boson mass we take $M_W = 80.425$ GeV [16]. The charged-current structure functions are given by

$$F_1^{\nu, \text{CC}}(x, Q^2) = \sum_{qq'} [q(x_{q'}, Q^2) + \bar{q}'(x_q, Q^2)] |V_{\text{CKM}}^{qq'}|^2, \quad (8)$$

$$F_1^{\bar{\nu}, \text{CC}}(x, Q^2) = \sum_{qq'} [\bar{q}(x_{q'}, Q^2) + q'(x_q, Q^2)] |V_{\text{CKM}}^{qq'}|^2, \quad (9)$$

$$F_2^{\nu, \text{CC}}(x, Q^2) = 2 \sum_{qq'} [x_{q'} q(x_{q'}, Q^2) + x_q \bar{q}'(x_q, Q^2)] |V_{\text{CKM}}^{qq'}|^2, \quad (10)$$

$$F_2^{\bar{\nu}, \text{CC}}(x, Q^2) = 2 \sum_{qq'} [x_{q'} \bar{q}(x_{q'}, Q^2) + x_q q'(x_q, Q^2)] |V_{\text{CKM}}^{qq'}|^2, \quad (11)$$

$$F_3^{\nu, \text{CC}}(x, Q^2) = 2 \sum_{qq'} [q(x_{q'}, Q^2) - \bar{q}'(x_q, Q^2)] |V_{\text{CKM}}^{qq'}|^2, \quad (12)$$

$$F_3^{\bar{\nu}, \text{CC}}(x, Q^2) = 2 \sum_{qq'} [q'(x_q, Q^2) - \bar{q}(x_{q'}, Q^2)] |V_{\text{CKM}}^{qq'}|^2, \quad (13)$$

where the quark flavour indices run through $q = d, s, b$ and $q' = u, c$. The momentum fraction $x_q \equiv x(1 + \frac{m_q^2}{Q^2})$ accounts for the mass of the produced heavy quark. We consider u and d quarks massless and take $m_c = 1.2$ GeV and $m_b = 4.3$ GeV. We

also set $q(x_q, Q^2) = 0$ when $x_q \geq 1$. In the initial state, the quark masses are ignored here, as is the case in the scale evolution of the PDFs, too. The Cabibbo-Kobayashi-Maskawa mixing matrix elements are denoted by $V_{\text{CKM}}^{qq'}$. In what follows, we shall use $V_{\text{CKM}}^{du} = 0.97458$, $V_{\text{CKM}}^{dc} = 0.224$, $V_{\text{CKM}}^{su} = 0.224$, $V_{\text{CKM}}^{sc} = 0.9738$, $V_{\text{CKM}}^{bu} = 0.003$, $V_{\text{CKM}}^{bc} = 0.04$, taken from [16].

For forming the Paschos-Wolfenstein ratios in Eqs. (1) and (2), we form the differences of the above neutrino and antineutrino cross sections,

$$\frac{d\sigma^{\nu, \text{NC}}}{dx dQ^2} - \frac{d\sigma^{\bar{\nu}, \text{NC}}}{dx dQ^2} = \frac{G_F^2}{\pi} \left(\frac{M_Z^2}{M_Z^2 + Q^2} \right)^2 \frac{1}{8x} xy \left(1 - \frac{y}{2} \right) 2F_3^{\nu(\bar{\nu}), \text{NC}}(x, Q^2), \quad (14)$$

$$\begin{aligned} \frac{d\sigma^{\nu, \text{CC}}}{dx dQ^2} - \frac{d\sigma^{\bar{\nu}, \text{CC}}}{dx dQ^2} &= \frac{G_F^2}{\pi} \left(\frac{M_W^2}{M_W^2 + Q^2} \right)^2 \frac{1}{2x} \left[xy^2 \Delta F_1^{\text{CC}}(x, Q^2) \right. \\ &\quad \left. + \left(1 - y - \frac{mxy}{2E} \right) \Delta F_2^{\text{CC}}(x, Q^2) + xy \left(1 - \frac{y}{2} \right) \Sigma F_3^{\text{CC}}(x, Q^2) \right], \end{aligned} \quad (15)$$

where we define

$$\begin{aligned} \Delta F_1^{\text{CC}}(x, Q^2) &\equiv F_1^{\nu, \text{CC}}(x, Q^2) - F_1^{\bar{\nu}, \text{CC}}(x, Q^2) \\ &= \sum_{qq'} [q_V(x_{q'}, Q^2) - q'_V(x_q, Q^2)] |V_{\text{CKM}}^{qq'}|^2, \end{aligned} \quad (16)$$

$$\begin{aligned} \Delta F_2^{\text{CC}}(x, Q^2) &\equiv F_2^{\nu, \text{CC}}(x, Q^2) - F_2^{\bar{\nu}, \text{CC}}(x, Q^2) \\ &= 2 \sum_{qq'} [x_{q'} q_V(x_{q'}, Q^2) - x_q q'_V(x_q, Q^2)] |V_{\text{CKM}}^{qq'}|^2, \end{aligned} \quad (17)$$

$$\begin{aligned} \Sigma F_3^{\text{CC}}(x, Q^2) &\equiv F_3^{\nu, \text{CC}}(x, Q^2) + F_3^{\bar{\nu}, \text{CC}}(x, Q^2) \\ &= 2 \sum_{qq'} [q_V(x_{q'}, Q^2) + q'_V(x_q, Q^2)] |V_{\text{CKM}}^{qq'}|^2, \end{aligned} \quad (18)$$

where again the quark flavour indices run through $q = d, s, b$ and $q' = u, c$.

3 nPDFs and R_A^-

We define the quark PDFs $Q_A(x, Q^2)$ in a nucleus of mass number A and proton number Z as in the EKS98 global DGLAP analysis [13]. Denoting the number density distribution of the quark flavour q in a bound proton by $q^{p/A}(x, Q^2)$, and the corresponding parton distribution function in a bound neutron by $q^{n/A}(x, Q^2)$, the average number density of a quark q in the nucleus is

$$Q_A(x, Q^2) = Z q^{p/A}(x, Q^2) + (A - Z) q^{n/A}(x, Q^2), \quad (19)$$

Since we shall consider isospin effects below, it is useful to separate the symmetric and antisymmetric parts in the PDFs in the bound proton and neutron as

$$Q_A(x, Q^2) = \frac{A}{2} [q^{p/A}(x, Q^2) + q^{n/A}(x, Q^2)] + \frac{\Delta_A}{2} [q^{n/A}(x, Q^2) - q^{p/A}(x, Q^2)], \quad (20)$$

where the neutron excess is denoted as $\Delta_A \equiv A - 2Z$. In particular, as in EKS98, we define the nuclear PDFs to be those of the bound protons,

$$q_A(x, Q^2) \equiv q^{p/A}(x, Q^2), \quad (21)$$

and define their nuclear modifications relative to the corresponding PDFs in the free proton,

$$q_A(x, Q^2) \equiv R_q^A(x, Q^2)q(x, Q^2). \quad (22)$$

Again as in the EKS98 analysis [13], we assume that isospin symmetry between the bound protons and neutrons holds for arbitrary A , i.e. $u^{n/A} = d^{p/A}$, $d^{n/A} = u^{p/A}$, and similarly for \bar{u} and \bar{d} . For mirror symmetric nuclei (which of course includes isoscalars), this gives the standard isospin symmetric way of treating the PDFs in protons and neutrons. Thus, in the EKS98-framework adopted here, the isospin effects in the average quark distributions Q_A are always proportional to the neutron excess Δ_A and to the difference between the $u(\bar{u})$ and $d(\bar{d})$ quark(antiquark) distributions in a bound proton, while the possible difference between e.g. the u quark distribution in a proton of a nucleus ${}^N_Z A$ and the u quark distribution in a proton of its mirror nucleus ${}^Z_N A$ is neglected. In other words, the EKS98 nuclear effects in the bound proton PDFs depend only on A , not on Z . The scope of the presently existing data does not allow for a more detailed study of these effects. In practice, however, since we are dealing only with close-to-isoscalar nuclei, such as iron ($A = 56$, $Z = 26$) here, the isospin-symmetry-related approximation made can be expected to be a very good one.

In particular, below we shall discuss the average valence quark modification,

$$R_V^A(x, Q^2) \equiv \frac{u_V^A(x, Q^2) + d_V^A(x, Q^2)}{u_V(x, Q^2) + d_V(x, Q^2)}, \quad (23)$$

in terms of individual modifications for the the valence u quarks and valence d quarks,

$$R_{uV}^A(x, Q^2) \equiv \frac{u_V^A(x, Q^2)}{u_V(x, Q^2)}, \quad (24)$$

$$R_{dV}^A(x, Q^2) \equiv \frac{d_V^A(x, Q^2)}{d_V(x, Q^2)}. \quad (25)$$

Only two of these ratios are independent, so that e.g.

$$R_{uV}^A(x, Q^2) = R_V^A(x, Q^2) \frac{u_V(x, Q^2) + d_V(x, Q^2)}{u_V(x, Q^2)} - R_{dV}^A(x, Q^2) \frac{d_V(x, Q^2)}{u_V(x, Q^2)}. \quad (26)$$

Analogously to the global DGLAP fits of the free proton PDFs, in the global DGLAP fits for the nPDFs [13, 17, 18], the modification ratios $R_i^A(x, Q_0^2)$, $i = g, q$ at an initial scale Q_0^2 are iteratively determined based on fits to the deep inelastic lA scattering data and the Drell-Yan dilepton data from pA collisions. Also conservation

of baryon number, charge and momentum are accounted for. The amount and precision of the existing data do not, however, allow for a precise determination of the modifications $R_{u_V}^A$ and $R_{d_V}^A$ individually but for simplicity in [13, 17, 18] it is assumed that at the initial scale $R_{u_V}^A = R_{d_V}^A = R_V^A$. Once this assumption is made, the DGLAP scale evolution does not cause large deviations from it, and to a good approximation $R_{u_V}^A = R_{d_V}^A = R_V^A$ holds for scales $Q^2 \geq Q_0^2$ as well, see EKS98 [13]. The most recent efforts [9, 10, 11, 12] to disentangle the nuclear effects in u_V and d_V individually based on DIS and DY data do not lend support to significant differences between $R_{u_V}^A$ and $R_{d_V}^A$, either.

Below, we shall study to what extent the NuTeV $\sin^2 \theta_W$ anomaly could be explained by releasing this approximation, i.e. by considering mutually different $R_{u_V}^A$ and $R_{d_V}^A$ but keeping their relative magnitude such that the EKS98-value of average valence modification, R_V^A , is always reproduced, as in Eq. (26). In particular, we shall explore an extreme case where the whole NuTeV anomaly is accounted for by changes in $R_{u_V}^A$ and $R_{d_V}^A$, and study the possible consequences for the global DGLAP fits.

To demonstrate the nuclear effects in the PW ratio $R_A^-(x)$, and to see the systematics expected, we first consider the ratio $R_A^-(x, Q^2)$ in an approximation, where only u and d quarks are active, $V_{\text{CKM}}^{du} = 1$, virtualities are modest, $Q^2 \ll M_Z^2, M_W^2$, and beam energy is so high that the term $xy/(2E)$ in Eqs. (3) and (7) can be ignored. Using the nPDF definitions above, we obtain for the neutral current case

$$F_{3,A}^{\nu,\text{NC}}(x, Q^2) = A(2 - 4x_W) \left[u_V^A(x, Q^2) + d_V^A(x, Q^2) \right] + \Delta_A \frac{4}{3} x_W \left[u_V^A(x, Q^2) - d_V^A(x, Q^2) \right] \quad (27)$$

and for the charged current case

$$\Delta F_{1,A}^{\text{CC}}(x, Q^2) = \Delta_A \left[u_V^A(x, Q^2) - d_V^A(x, Q^2) \right] = \frac{1}{2x} \Delta F_2^{\text{CC}}(x, Q^2) \quad (28)$$

$$\Sigma F_{3,A}^{\text{CC}}(x, Q^2) = 2A \left[u_V^A(x, Q^2) + d_V^A(x, Q^2) \right]. \quad (29)$$

Substituting these into Eqs. (14) and (15) and forming the PW ratio in Eq. (1), we arrive at

$$R_A^-(x, Q^2) = \left(\frac{1}{2} - x_W \right) \left(1 + \frac{\Delta_A}{A} \frac{2x_W}{3 - 6x_W} \frac{u_V^A - d_V^A}{u_V^A + d_V^A} \right) \left(1 + \frac{\Delta_A}{A} \frac{1 + (1 - y)^2}{1 - (1 - y)^2} \frac{u_V^A - d_V^A}{u_V^A + d_V^A} \right)^{-1}, \quad (30)$$

where the arguments x, Q^2 are implicit in the nPDFs on the r.h.s.

For isoscalar nuclei, $\Delta_A = 0$, one obtains the conventional result, $R_{A_{\text{iso}}}^- = 1/2 - x_W$. For non-isoscalar nuclei, isospin corrections proportional to Δ_A/A arise. We also immediately see that in the PW ratio of differential cross sections, $R_A^-(x, Q^2)$, the effects of nuclear valence quark modifications cancel out if the modifications are the same both for the nuclear valence- u and for valence- d quark distributions.

We compute the PW ratio in two different ways:

1. For $R_A^-(x, Q^2; x_W^{\text{NuTeV}}, R_{d_V}^A = R_{u_V}^A = R_V^A)$, we use the NuTeV value $x_W^{\text{NuTeV}} = 0.2277$ and take the *same* modification R_V^A from EKS98 for both $R_{u_V}^A$ and $R_{d_V}^A$.

2. For $R_A^-(x, Q^2; \langle x_W \rangle, R_{d_V}^A \neq R_{u_V}^A)$, we apply the world average value $\langle x_W \rangle = 0.2227$ and assume $R_{u_V}^A \neq R_{d_V}^A$.

Setting these two PW ratios equal should then give us an idea into which direction the nuclear modifications $R_{u_V}^A$ and $R_{d_V}^A$ should deviate from the average valence modification R_V^A so that the change in the PW ratio caused by the larger NuTeV value of x_W is accounted for.

Since the y values we shall consider below, are always larger than 0.1 and Δ_A/A is of the order 0.1 for iron and $(u_V^A - d_V^A)/(u_V^A + d_V^A) \ll 1$, we can expand the denominator in Eq. (30). This gives

$$R_A^-(x, Q^2, x_W) \approx \left(\frac{1}{2} - x_W\right) \left\{ 1 - \frac{\Delta_A}{A} h(y, x_W) \frac{u_V^A - d_V^A}{u_V^A + d_V^A} \right\} \quad (31)$$

where $h(y, x_W) \equiv \frac{1+(1-y)^2}{1-(1-y)^2} - \frac{2x_W}{3-6x_W}$ is always positive and not sensitive to small changes of x_W , since the first term dominates. Now, we set

$$R_A^-(x, Q^2; x_W^{\text{NuTeV}}, R_{d_V}^A = R_{u_V}^A = R_V^A) = R_A^-(x, Q^2; \langle x_W \rangle, R_{d_V}^A \neq R_{u_V}^A) \quad (32)$$

which, since $x_W^{\text{NuTeV}} > \langle x_W \rangle$, leads to

$$\frac{u_V - d_V}{u_V + d_V} < \frac{u_V^A - d_V^A}{u_V^A + d_V^A}, \quad (33)$$

where the nuclear effects on the l.h.s. have cancelled each other. Then, applying the definitions in Eqs. (23)-(26) to the nuclear PDFs indicates that

$$R_{d_V}^A(x, Q^2) < R_V^A(x, Q^2) < R_{u_V}^A(x, Q^2) \quad (34)$$

in the x, Q^2 region that the NuTeV cross sections are sensitive to.

4 Results

Let us now turn to a more detailed quantitative study of the PW ratio $R_A^-(x)$ in Eq. (2). In the NuTeV experiment [1], the neutrino and antineutrino cross sections were measured over a range of beam energies, virtualities Q^2 and Bjorken- x . Also cuts in the calorimeter energy were done. We do not attempt to simulate the kinematics in the experimentally collected event sample here in detail. Instead, we simply fix the beam energy to $E = 116$ GeV, close to the NuTeV's average neutrino and antineutrino beam energies and the virtuality to $Q^2 = 20.5$ GeV², corresponding to the NuTeV's average virtuality and integrate over x in forming the PW ratio in Eq. (2). To mimic the NuTeV cuts on the calorimeter energy, we require the final state energy on the hadron-remnant side to be in the range $E_{\min} \leq m + yE \leq E_{\max}$, with $E_{\min} = 20$ GeV

and $E_{\max} = 180$ GeV. This, together with the requirement $y = Q^2/(2mEx) \leq 1$, fixes the integration limits for x as

$$0.094 \approx \frac{Q^2}{2mE} = x_{\min} \leq x \leq x_{\max} = \frac{Q^2}{2m(E_{\min} - m)} \approx 0.57. \quad (35)$$

We emphasize, however, that exact kinematic limits are somewhat irrelevant from the point of view of this paper. We aim to study whether order-of-magnitude changes in the nuclear modifications would be needed in order to explain the NuTeV anomaly in a very conventional manner. We shall show that in fact surprisingly modest modifications, of the order 20-30 %, are sufficient. In the following, all the results are for iron nucleus $A = 56$ and $\Delta_A = 4$.

In Fig. 1 we show the differences of the double differential neutrino and antineutrino cross sections from Eqs. (14) and (15) as a function of x , computed with $\langle x_W \rangle$, and CTEQ6L [19] PDFs with $R_{d_V}^A = R_{u_V}^A = R_V^A$ from EKS98 [13]. From the result, it is obvious that the smallest- x region dominates in the x -integrated cross sections. Thus, we should be looking for modifications of $R_{d_V}^A$ and $R_{u_V}^A$ in the region $x \gtrsim x_{\min} \sim 0.1$.

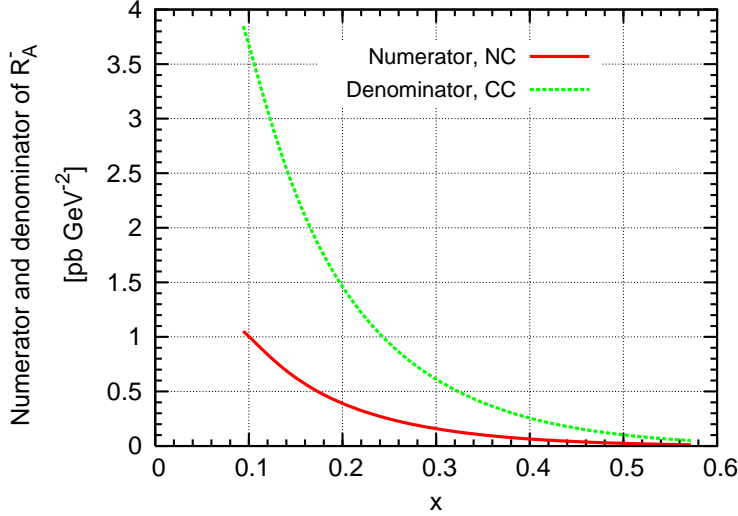


Figure 1: The cross section differences $d\sigma_A^{\nu, \text{NC}}/dx dQ^2 - d\sigma_A^{\bar{\nu}, \text{NC}}/dx dQ^2$ and $d\sigma_A^{\nu, \text{CC}}/dx dQ^2 - d\sigma_A^{\bar{\nu}, \text{CC}}/dx dQ^2$ as a function of x computed from Eqs. (14) and (15) at $Q^2 = 20.5$ GeV and $E = 116$ GeV, with EKS98 [13] nuclear PDF effects for iron, $A = 56$, $Z = 26$, and using the world average value of mixing angle $\langle x_W \rangle = 0.2227$.

To get transparent order-of-magnitude estimates of the individual modifications $R_{d_V}^A$ and $R_{u_V}^A$ in light of the NuTeV $\sin^2 \theta_W$ anomaly, we assume the following very rough form for the valence- d quark modification in iron at $Q^2 = 20.5$ GeV² (see Fig. 3

ahead) :

$$R_{d_V}^A(x, Q^2) = \begin{cases} C_1 = \text{constant}, & \text{when } x < x_{\min} \\ C_2 = \text{constant}, & \text{when } x_{\min} \leq x \leq x_{\max} \\ R_V^A(x, Q^2) \text{ from EKS98} & \text{when } x_{\max} \leq x \leq 1 \end{cases} \quad (36)$$

For a fixed constant C_2 , the constant C_1 is determined from charge conservation $\int_0^1 dx d_V^A(x, Q^2) = 1$, after which the ratio $R_{u_V}^A$ is obtained from $R_V^A(\text{EKS98})$ and $R_{d_V}^A$ according to Eq. (26). Then, as the EKS98-result for R_V^A conserves baryon number, charge conservation $\int_0^1 dx u_V^A(x, Q^2) = 2$ is automatic. We proceed as outlined in the previous section. By using the x -integrated cross sections, we compute the PW ratios according to Eq. (2), on one hand for x_W^{NuTeV} and setting $R_{d_V}^A = R_{u_V}^A = R_V^A$, and on the other hand for $\langle x_W \rangle$ and setting $R_{d_V}^A \neq R_{u_V}^A$. The requirement (analogous to Eq. (32))

$$R_A^-(Q^2, x_W^{\text{NuTeV}}, R_{d_V}^A = R_{u_V}^A = R_V^A) = R_A^-(Q^2, \langle x_W \rangle, R_{d_V}^A \neq R_{u_V}^A), \quad (37)$$

now fixes the constant $C_2 \approx 0.708$ in $R_{d_V}^A$, and consequently $C_1 \approx 1.16$. Figure 2 shows the PW ratio as a function of the weak mixing angle, computed with the mutually different nuclear modifications $R_{d_V}^A$ and $R_{u_V}^A$ (r.h.s. of Eq. (37), "extreme"), and with the EKS98 modification R_V^A only (l.h.s. of Eq. (37), "EKS98").

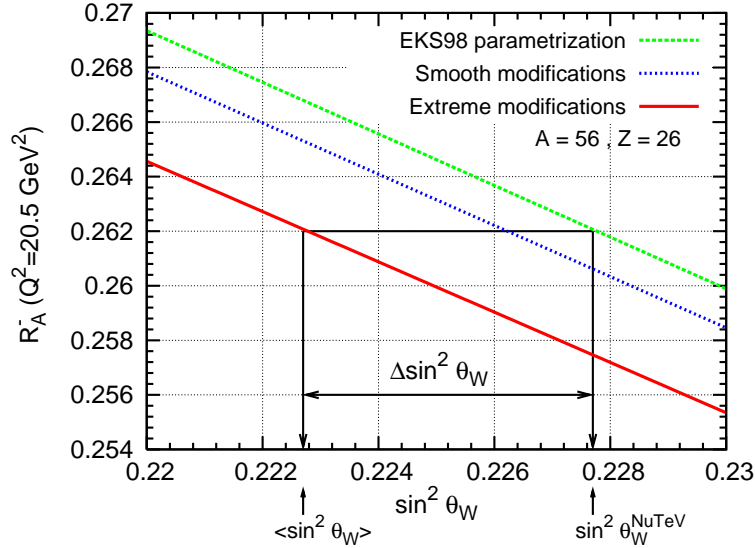


Figure 2: The Paschos-Wolfenstein ratio as a function of the weak mixing angle, computed for iron, $A = 56$, $Z = 26$, by identifying the individual nuclear modifications $R_{u_V}^A$ and $R_{d_V}^A$ with the EKS98 R_V^A , with those in Fig. 3 ("extreme"), and with those in Fig. 4 ("smooth"). The world average $\langle x_W \rangle$ and the NuteV result x_W^{NuTeV} are indicated.

Fig. 3, showing the extreme case where the mutually different nuclear modifications to u_V and d_V explain the whole NuTeV anomaly, is the main result of this paper. Perhaps somewhat surprisingly, our result shows that even if we do not invoke any exotic

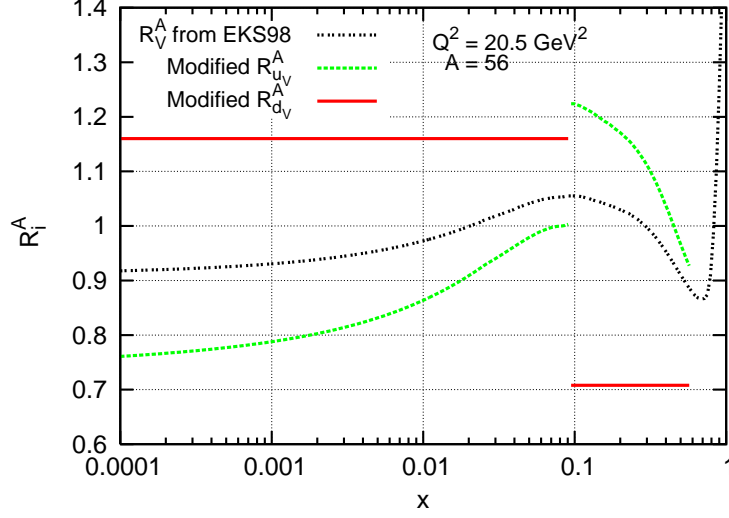


Figure 3: An order of magnitude estimate of the nuclear valence quark modifications needed to alone account for the large value of x_W reported by NuTeV. The individual modifications $R_{u_V}^A$ and $R_{d_V}^A$ are shown for iron, $A = 56$, $Z = 26$, as functions of x at a fixed scale $Q^2 = 20.5 \text{ GeV}^2$. The average valence quark modification R_V^A is from the EKS98-parametrization [13]. Definitions of the ratios R_i^A are given in Eqs. (23)-(25).

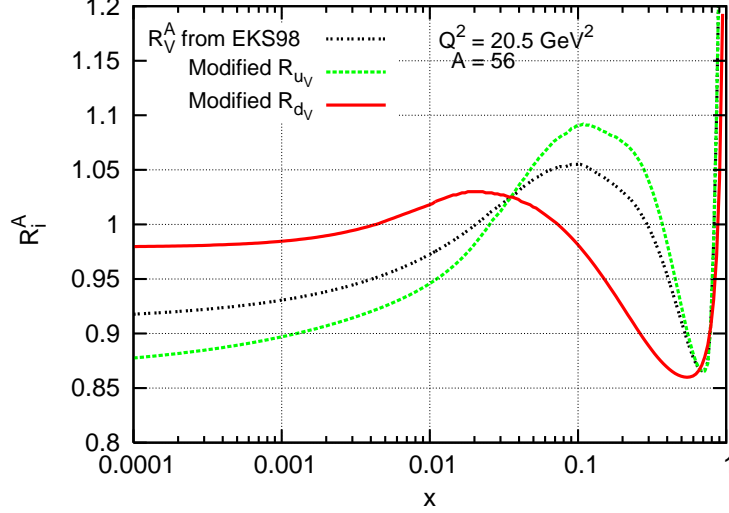


Figure 4: As Fig. 3 but an example of a case where only one third of the difference $x_W^{\text{NuTeV}} - \langle x_W \rangle$ would be explained.

new phenomena, such as isospin-breaking PDFs, locally non-zero $s - \bar{s}$ distributions, not to mention beyond-Standard-Model physics, to explain the NuTeV anomaly, fairly modest, $\sim 20 - 30$ % changes in the nuclear valence quark modifications would seem to explain the large value of x_W observed by NuTeV.

In addition to the extreme case considered above, we also consider, as an example, more modest changes with a continuous and smooth parametrization for $R_{d_V}^A$ shown in Fig. 4. Also here charge is conserved and the EKS98 ratio R_V^A is reproduced as explained above. Proceeding again in the same manner as above, we find that these nuclear effects would correspond to $x_W = 0.2243$, which would explain a third of the NuTeV anomaly $\Delta x_W = 0.005$.

5 Effects on $R_{F_2}^A$ and R_{DY}^A

Next, we show that the modifications $R_{u_V}^A$ and $R_{d_V}^A$ obtained above do not induce severe modifications into the quantities which are already rather well constrained in the global DGLAP analyses of nPDFs. As mentioned above, the data constraints are given by the lA DIS cross sections and Drell-Yan dilepton cross sections in pA collisions.

In DIS of leptons off the free proton, the leading order structure functions are

$$F_2^{lp}(x, Q^2) = \sum_q e_q^2 x \left[q(x, Q^2) + \bar{q}(x, Q^2) \right] = 2x F_1^{lp}(x, Q^2). \quad (38)$$

The nuclear modifications of F_2^{lA} are specified relative to deuterium,

$$R_{F_2}^A(x, Q^2) \equiv \frac{\frac{1}{A} d\sigma^{lA}/dx dQ^2}{\frac{1}{2} d\sigma^{lD}/dx dQ^2} = \frac{\frac{1}{A} F_2^{lA}(x, Q^2)}{\frac{1}{2} F_2^{lD}(x, Q^2)}, \quad (39)$$

Then, as discussed in [13], and using the definitions of nPDFs given here, the nuclear modifications of F_2^{lA} relative to deuterium become (suppressing the arguments x, Q^2)

$$R_{F_2}^A = \frac{5(u_A + d_A + \bar{u}_A + \bar{d}_A) + 4(s_A + \bar{s}_A) + \dots + \frac{3\Delta_A}{A}(d_A + \bar{d}_A - u_A - \bar{u}_A)}{5(u + d + \bar{u} + \bar{d}) + 4(s + \bar{s}) + \dots}, \quad (40)$$

where the dots denote the heavy quark contributions and the small nuclear effects in deuterium have been neglected. From above, we see that since $u_A + d_A = u_V^A + d_V^A + \bar{u}_A + \bar{d}_A = R_V^A(u_V + d_V) + \bar{u}_A + \bar{d}_A$, any change in $R_{u_V}^A$ and $R_{d_V}^A$ that leaves the valence modification R_V^A unchanged, will not at all change the isoscalar part. We emphasize that the DIS lA data has usually been approximately "isospin-symmetrized" by the experimental collaborations. E.g. the EKS98 analysis is using such isospin-symmetrized DIS data (NMC, SLAC mainly) and therefore in constraining the fits, one is only discussing isospin symmetric nuclei for DIS. We show in Fig. 5 the effects that our extreme modifications of $R_{d_V}^A$ and $R_{u_V}^A$ in Fig. 3 would induce into the ratio $R_{F_2}^A$ of non-isoscalar iron at $Q^2 = 20.5 \text{ GeV}^2$. Since the changes due to $R_{d_V}^A \neq R_{u_V}^A$ only take place in the subleading correction term proportional to Δ_A/A , the effects remain

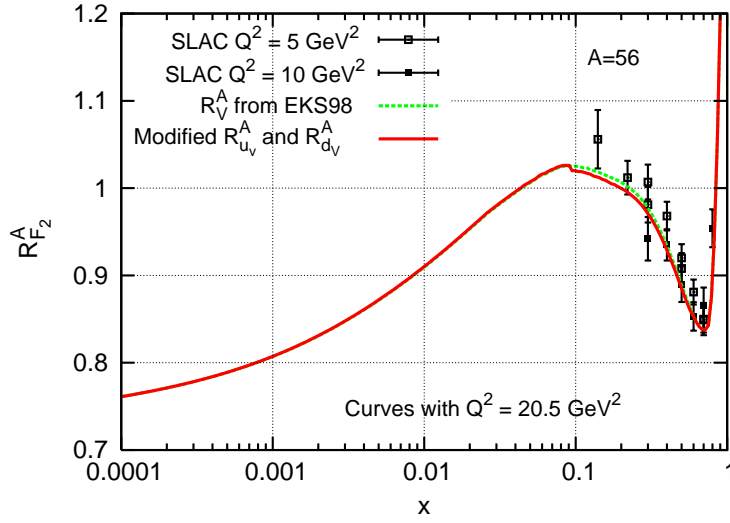


Figure 5: The nuclear modification ratio $R_{F_2}^A$ for non-isospin-symmetrized iron, $A = 56$ and $Z = 26$, as a function of x at a fixed scale $Q^2 = 20.5 \text{ GeV}^2$. The dashed curve is computed with the EKS98 modifications and the solid one is the result when the extreme modifications of Fig. 3 are applied for $R_{u_V}^A$ and $R_{d_V}^A$. The SLAC data shown have been isospin symmetrized [21].

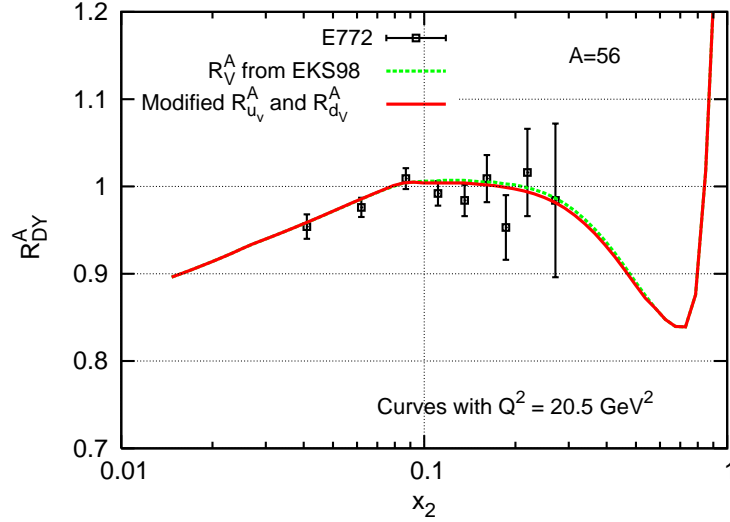


Figure 6: The nuclear modification ratio $R_{DY}^A(x_2, Q^2)$ for non-isospin-symmetrized iron, $A = 56$ and $Z = 26$, as a function of the target-side momentum fraction x_2 at a fixed scale $Q^2 = 20.5 \text{ GeV}^2$. The dashed curve is computed with the EKS98 modifications and the solid one is the result when the extreme modifications of Fig. 3 are used for $R_{u_V}^A$ and $R_{d_V}^A$. The data shown are from E772 [20].

very small, below one per cent level for iron. Given the precision of the existing data, such small changes can be easily accommodated in the global DGLAP fits.

Finally, we perform a similar check for the Drell-Yan nuclear modification ratio $R_{\text{DY}}^A(x_2, Q^2)$ (see [13]), which can be written in the LO as follows

$$\begin{aligned}
R_{\text{DY}}^A(x_2, Q^2) &\equiv \frac{\frac{1}{A} d\sigma^{pA}/dx_2 dQ^2}{\frac{1}{2} d\sigma^{pD}/dx_2 dQ^2} \\
&= \{4[u_1(\bar{u}_2^A + \bar{d}_2^A) + \bar{u}_1(u_2^A + d_2^A)] + [d_1(\bar{d}_2^A + \bar{u}_2^A) + \bar{d}_1(u_2^A + d_2^A)] + 4s_1 s_2^A + \dots\}/N_{\text{DY}} \\
&\quad + \frac{\Delta_A}{A} \{4[u_1(\bar{d}_2^A - \bar{u}_2^A) + \bar{u}_1(d_2^A - u_2^A)] + [d_1(\bar{u}_2^A - \bar{d}_2^A) + \bar{d}_1(u_2^A - d_2^A)]\}/N_{\text{DY}}, \quad (41)
\end{aligned}$$

where $N_{\text{DY}} = 4[u_1(\bar{u}_2 + \bar{d}_2) + \bar{u}_1(u_2 + d_2)] + [d_1(\bar{d}_2 + \bar{u}_2) + \bar{d}_1(u_2 + d_2)] + 4s_1 s_2 + \dots$ and Q^2 is the invariant mass of the lepton pair, and where we have used the notation $q_j^{(A)} \equiv q_{(A)}(x_j, Q^2)$ with $j = 1, 2$, where $x_2(x_1)$ is the fractional momentum of the colliding parton from the target (projectile). Again the quark combination $u_A + d_A$ appears in the leading, isoscalar, term. For isoscalars, any R_V^A -conserving changes made for $R_{u_V}^A$ and $R_{d_V}^A$ will not affect the ratio $R_{\text{DY}}^A(x_2, Q^2)$ at all. Contrary to the DIS case, however, the DY data available are not isospin-symmetrized but show also some isospin effects. The modifications of $R_{u_V}^A$ and $R_{d_V}^A$ will be transmitted to R_{DY}^A only through the correction term proportional to Δ_A/A and hence even the extreme modifications of Eq. (36) and Fig. 3 cause only a small deviation from the result computed with the EKS98 nuclear modifications. This is shown in Fig. 6, where we compute the ratio $R_{\text{DY}}^A(x_2, Q^2)$ as a function of x_2 at a fixed scale $Q^2 = 20.5 \text{ GeV}^2$ on one hand with the extreme modifications for $R_{u_V}^A$ and $R_{d_V}^A$ and on the other with the EKS98 modifications only. Again the difference to the EKS98-based result is less than a percent. We thus conclude that the DIS and DY cross sections used in the global DGLAP fits are essentially insensitive to the decomposition of R_V^A into $R_{u_V}^A$ and $R_{d_V}^A$, as long as the average valence quark modification remains unchanged. Thus, the interpretation of the NuTeV $\sin^2 \theta_W$ anomaly in terms of conventional physics, mutually different $R_{u_V}^A$ and $R_{d_V}^A$, does not lead into a contradiction with the existing global DGLAP fits for the nPDFs.

6 Effects on R_A^ν in NOMAD

As the final point in this paper, we make the following prediction for the NOMAD neutrino experiment at CERN [14]. In this experiment one can measure the ratio of charged current and neutral current neutrino-iron cross sections,

$$R^\nu \equiv \frac{\sigma_A^{\nu, \text{NC}}}{\sigma_A^{\nu, \text{CC}}}. \quad (42)$$

The differential cross sections are given in Eqs. (3) and (7). With the parameters $\langle Q^2 \rangle = 13 \text{ GeV}^2$ and $\langle E_\nu \rangle = 45.4 \text{ GeV}$, the typical NOMAD x -range becomes $x \gtrsim 0.15$.

This is close to that of NuTeV, and the valence quarks dominate the x -integrated cross sections. As shown in Fig. 7, we compute the x -integrated cross sections at a fixed scale $Q^2 = 13 \text{ GeV}^2$ and form the ratio R_A^ν again in two different ways: on one hand we apply the EKS98 nuclear effects, where $R_{u_V}^A = R_{d_V}^A = R_V^A$, and on the other we apply the individual modifications $R_{u_V}^A \neq R_{d_V}^A$ from Figs. 3 and 4 (and EKS98 for the parton flavours other than valence quarks). The figure demonstrates that the situation with R_A^ν in NOMAD should be very similar to that with the PW ratio in NuTeV: if identical nuclear corrections are used for u_V and d_V , the value of x_W extracted from the NOMAD data will be larger than the world average $\langle x_W \rangle$. If the whole NuTeV anomaly is explained by the individual, mutually different, nuclear effects in u_V and d_V distributions, then solving x_W^{NOMAD} from

$$R_A^\nu(Q^2, x_W^{\text{NOMAD}}, R_i^{A, \text{EKS98}}) = R_A^\nu(Q^2, \langle x_W \rangle, R_{i \neq u_V, d_V}^A = R_i^{A, \text{EKS98}}, R_{d_V}^A \neq R_{u_V}^A), \quad (43)$$

where the individual modifications $R_{d_V}^A$ and $R_{u_V}^A$ are the extreme ones from Fig. 3, gives $x_W^{\text{NOMAD}} \approx 0.2265$, i.e. $\Delta x_W^{\text{NOMAD}} = x_W^{\text{NOMAD}} - \langle x_W \rangle \approx 0.004$, close to the result obtained by NuTeV. With the smooth modifications in Fig. 4, the increase in x_W is again close to that obtained in Fig. 2.

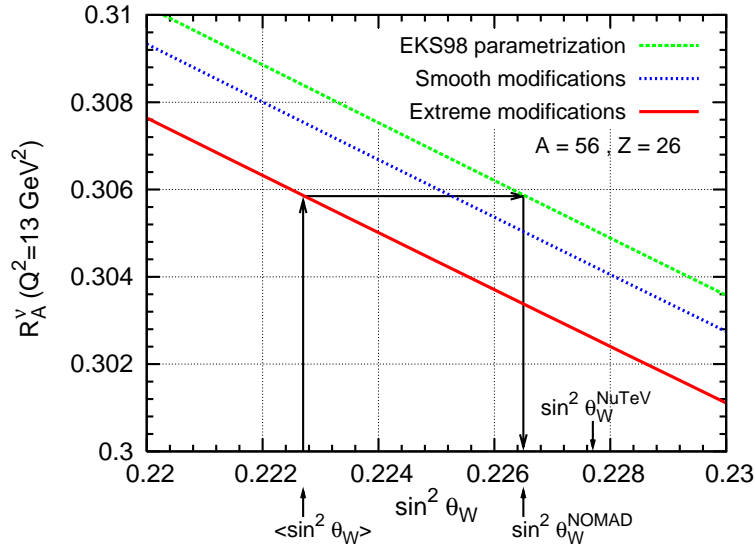


Figure 7: The ratio R_A^ν for iron, $A = 56, Z = 26$, as a function of $\sin^2 \theta_W$, computed in the x -range of NOMAD at $Q^2 = 13 \text{ GeV}^2$ with the EKS98 nuclear modifications ("EKS98"), with extreme individual nuclear modifications $R_{u_V}^A$ and $R_{d_V}^A$ in Fig. 3 together with the EKS98 for other parton flavours ("extreme"), and with the smooth modifications in Fig. 4 together with the EKS98 ("smooth"). The world average $\langle x_W \rangle$ and the expected increase of x_W in the NOMAD case, cf. Eq. (43), are indicated.

7 Conclusions

For the nuclear valence quark PDFs one usually makes the approximation $u_V^A/u_V \approx d_V^A/d_V \approx (u_V^A + d_V^A)/(u_V + d_V) \equiv R_V^A$. In this case, the effects from the nuclear valence quark modification R_V^A are cancelled out in the Paschos-Wolfenstein ratio $R^-(x, Q^2)$. In this paper, we are suggesting that taking $R_{u_V}^A \equiv u_V^A/u_V \neq d_V^A/d_V \equiv R_{d_V}^A$ and by allowing nuclear effects of the order of 30 %, leads to the modifications of the Paschos-Wolfenstein ratio $R^-(Q^2)$ which are as large as would be induced by increasing the weak mixing angle x_W to the large value reported by NuTeV. We have also checked that as long as the valence modification R_V^A is conserved in the decomposition into $R_{u_V}^A$ and $R_{d_V}^A$, the computed ratios of the nuclear DIS and DY cross sections over deuterium, used as data constraints in the global DGLAP analyses of nPDFs, change by less than a percent in the case of iron. On one hand, this insensitivity shows that the explanation of the NuteV anomaly in terms of nPDFs is well possible without running into contradiction with the global nPDF analyses. On the other hand, it shows, in agreement with [13, 9, 11], that in practice it is not possible to pin down the individual nuclear effects $R_{u_V}^A$ and $R_{d_V}^A$ based on finite-precision nuclear DIS and DY data. The main point of the present paper thus is that most, if not all, of the $\sin^2 \theta_W$ NuTeV anomaly could be explained by conventional physics and that the NuTeV result can play a key role in disentangling these effects for u_V and d_V . Finally, as a consequence, we predict that if the whole NuTeV anomaly can be accounted for by the nuclear corrections as we suggest here, and if identical nuclear effects for u_V and d_V are used in the data analysis, the value of $\sin^2 \theta_W$ to be determined in the NOMAD neutrino experiment at CERN should be quite close to that obtained by NuTeV.

We wish to emphasize that in the global nPDF analyses the shapes of the individual nuclear corrections to the PDFs are determined based on the data constraints (through DGLAP evolution) and sum rules. The origin of these corrections, and PDFs in general, is nonperturbative. If the NuTeV anomaly indeed is due to the nPDF effects as we suggest above, it would be very interesting to understand the mechanism which makes the nuclear effects for u_V and d_V distributions so different. We do not have an answer to this question for the moment.

In this paper, we do not make an attempt to simulate the NuTeV kinematics in detail but our goal is to show that interpretation of the NuTeV anomaly in terms of nPDF effects is indeed possible and to see the order of magnitude for the effects needed. The more detailed kinematics, along with scale evolution details of the valence quark effects, we shall consider elsewhere.

Acknowledgements. We thank P. Castorina, V. Ruuskanen and K. Tuominen for discussions. Financial support from the Academy of Finland, the Project No. 206024, is gratefully acknowledged.

References

- [1] G. P. Zeller *et al.* [NuTeV Collaboration], Phys. Rev. Lett. **88** (2002) 091802 [Erratum-ibid. **90** (2003) 239902] [arXiv:hep-ex/0110059].
- [2] D. Abbaneo *et al.* [ALEPH Collaboration], arXiv:hep-ex/0112021.
- [3] K. S. McFarland and S. O. Moch, arXiv:hep-ph/0306052.
- [4] S. Davidson, S. Forte, P. Gambino, N. Rius and A. Strumia, JHEP **0202** (2002) 037 [arXiv:hep-ph/0112302].
- [5] G. P. Zeller *et al.* [NuTeV Collaboration], Phys. Rev. D **65** (2002) 111103 [Erratum-ibid. D **67** (2003) 119902] [arXiv:hep-ex/0203004].
- [6] D. Mason [NuTeV Collaboration], arXiv:hep-ex/0405037.
- [7] S. Kretzer, F. Olness, J. Pumplin, D. Stump, W. K. Tung and M. H. Reno, Phys. Rev. Lett. **93** (2004) 041802 [arXiv:hep-ph/0312322].
- [8] S. Kovalenko, I. Schmidt and J. J. Yang, Phys. Lett. B **546**, 68 (2002) [arXiv:hep-ph/0207158].
- [9] S. Kumano, Phys. Rev. D **66** (2002) 111301 [arXiv:hep-ph/0209200].
- [10] M. Hirai, S. Kumano and T. H. Nagai, arXiv:hep-ph/0408023.
- [11] M. Hirai, S. Kumano and T. H. Nagai, Phys. Rev. D **71** (2005) 113007 [arXiv:hep-ph/0412284].
- [12] M. Hirai, S. Kumano and T. H. Nagai, arXiv:hep-ph/0601070.
- [13] K. J. Eskola, V. J. Kolhinen and P. V. Ruuskanen, Nucl. Phys. B **535** (1998) 351 [arXiv:hep-ph/9802350]; K. J. Eskola, V. J. Kolhinen and C. A. Salgado, Eur. Phys. J. C **9** (1999) 61 [arXiv:hep-ph/9807297].
<http://urhic.phys.jyu.fi/EKS98/EKS98param.html>
- [14] R. Petti [NOMAD Collaboration], arXiv:hep-ex/0411032.
- [15] E. A. Paschos and L. Wolfenstein, Phys. Rev. D **7** (1973) 91.
- [16] S. Eidelman *et al.* [Particle Data Group Collaboration], Phys. Lett. B **592** (2004) 1.
- [17] M. Hirai, S. Kumano and M. Miyama, Phys. Rev. D **64** (2001) 034003 [arXiv:hep-ph/0103208].
- [18] D. de Florian and R. Sassot, Phys. Rev. D **69** (2004) 074028 [arXiv:hep-ph/0311227].

- [19] J. Pumplin, D. R. Stump, J. Huston, H. L. Lai, P. Nadolsky and W. K. Tung, JHEP **0207** (2002) 012 [arXiv:hep-ph/0201195].
- [20] D. M. Alde *et al.*, Phys. Rev. Lett. **64** (1990) 2479.
- [21] J. Gomez *et al.*, Phys. Rev. D **49** (1994) 4348.